Circadian Light Source Based on K x Na 1-x LuS 2 :Eu 2+ Phosphor

Vítězslav Jary, Lubomír Havlák, Jan Bárta, Martin Rejman, Aleš Bystřicky, Christophe Dujardin, Gilles Ledoux, Martin Nikl

JSS Focus Issue on Visible and Infrared Phosphor Research and Applications

Circadian Light Source Based on $K_xNa_{1-x}LuS_2:Eu^{2+}$ Phosphor

Vítězslav Jarý,[a,z] Lubomír Havlák,[a] Jan Bárta,[a,b] Martin Rejman,[a] Aleš Bystřický,[a] Christophe Dujardin,[c] Gilles Ledoux,[c] and Martin Nikl[a]

[a]*Institute of Physics, Czech Academy of Sciences in Prague, 18240 Prague 8, Czech Republic*
[b]*Faculty of Nuclear Sciences and Physical Engineering, Czech Technical University in Prague, 11519 Prague 1, Czech Republic*
[c]*Institut Lumière Matière ILM UMR5306 Université Lyon 1/CNRS, Université de Lyon, 69622 Villeurbanne Cedex, France*

The presented work describes a functional demonstration device representing the source of white light with tunable color correlated temperature. Tunability is achieved by using two different kinds of excitation diodes (nearUV and blue) in combination with a proper $K_xNa_{1-x}LuS_2:Eu^{2+}$ phosphor. Its luminescence due to the Eu^{2+} 5*d*–4*f* allowed transition covers a broad emission region in visible range under both nearUV and blue excitations. The possibility to change the intensity ratio of the excitation diodes yields the changes of the output color correlated temperature. These changes are clearly demonstrated by shifts in the CIE color space; light quality is also quantified and discussed using CRI (color rendering index) and CQS (color quality scale) metrics.

Manuscript submitted August 3, 2017; revised manuscript received September 13, 2017. Published October 27, 2017. *This paper is part of the JSS Focus Issue on Visible and Infrared Phosphor Research and Applications.*

Solid state lighting (SSL) is a pivotal emerging technology promising to fundamentally alter and improve future lighting systems.[1] The impetus to SSL is provided by its following attractive features: Energy efficiency, possibility of safe battery-driven operation (LED operation does not require high voltage), emission of light of an intended color without using color filters, decreased heat generation (LED lamps are based on the cold emission of light as LED beam is without any infrared content), environment friendliness (free of hazardous substances found in conventional lamp technologies). LED lighting also eliminates noise pollution by avoiding the humming, flickering and headaches related to fluorescent lighting and provides higher reliability, extended lifetime and long-term cost-effectiveness (due to absence of moving parts, LED provides a high breakage and vibration resistance, hence, the sudden premature failures are unlikely). The rated lifetime of LEDs is usually around 60,000 h as opposed to 1,000–2,000 h for incandescent lamps and about 5,000–10,000 h for compact fluorescent lights). Other advantages comprise instant ON/OFF switching, suitability for frequent on-off cycling applications, equipment size and weight reduction due to small LED form factor, adjustment flexibility, elimination of sun phantom effect, extensive applications.[2–6]

Tunable-white lighting is one of the biggest trends in commercial lighting.[7] LED developers have taken a serious grip on the photobiological research being produced by university departments and other groups. We know more about the way that human bodies function than ever before and the science appears to support a practical technology that is perfectly suited to LED exploitation. Tunable white light products can mix warm and cool white light and light intensity so that it mimics outdoor lighting conditions (where morning light has different color and intensity than midday light). This promotes feeling of well-being and productivity for people who spend big part of their day indoors in artificial light, e.g. office workers, school students, hospital patients, etc.[8]

Standard LED color-mixing uses red (R), green (G) and blue (B) channels that are adjusted to deliver the entire range of the color spectrum. RGB LED products combine these three colors to produce over 16 million hues of light, but not all colors are possible using this approach. Some colors are "outside" the triangle (gamut) formed by the RGB LEDs. Also, pigment colors such as brown or pink are difficult, or impossible, to achieve. Tunable-whites work in a similar way, using a number of controllable channels to adjust the color temperature of the luminaries' white light output. The channels in a tunable-white system all produce white light, but with varying color temperatures, from a warm tone to a cool tone. Inevitably, there are levels of sophistication involved in tunable-white systems. The most basic tunable linear systems use LED strips mounted side-by-side. One channel is close to 2700 K in color temperature, with the other is up around a cool 6000 K. The LED strips are mounted inside an aluminum extrusion fitted with an opal diffuser, which does the color mixing as the light passes through it. It is very simple from the engineering point of view, but satisfies only the basic market with its low performance expectations. More products are using 'multi-chips' where a number of tiny LED chips are combined into the same module. This means that the color mixing occurs as the light leaves the module. Their very small size means that tunable-white products can be made much smaller, so we are starting to see downlights using the technology as well as linear systems. These multi-chips tend to have higher performance specification than the individual LED strips. Cheaper products may advertise good color performance at the extremes of the tunable range, where light is being delivered from either the warm or the cool channel, but there is no certainty that the mixed light performs equally well. Generally speaking, the greater the number of channels (the systems vary from two-channel to five-channel), the better the color rendering. Some systems offer a wide natural 'circadian rhythm' range that shifts from candlelight to daylight; there are also other systems with a much smaller range, from 2500 K to 4000 K, which should only be considered as a decorative option.[7] The most sophisticated control strategies are designed to manipulate the circadian rhythm of room occupants. This means that the lighting settings are programmed into the control architecture. Shifts in color temperature and light level can be pre-set or can be instigated by a manual over-ride. This is the method that is being used in recent school installations in Scandinavia, for example.[9]

It has been pointed out that not all 'tunable-white' mixing requires a full color range. Complex tunable-white schemes mean that one should be able to call up any CCT temperature within the mixing range. But some clients will call for specific CCT temperatures, often those that are commercially available, such as 3000 K, 4000 K, 6500 K. If that is the case, then it may be simpler–and cheaper–to consider having three discrete lighting channels operating separately within a bespoke housing.[7]

In the phosphors, the doping of host material by Eu^{2+} ion can offer very interesting emitted light characteristics. The energy position of Eu^{2+} $4f^{N-1}5d^1$ level and $4f^N \rightarrow 4f^{N-1}5d^1$ transitions in inorganic hosts is modified by the covalency and polarizability of Eu^{2+}-ligand bonds.

[z]E-mail: jary@fzu.cz

Table I. Compositions of mixtures used for the synthesis of $K_{1-x}Na_xLuS_2$:Eu crystals.

Sample assignment (arbitrary)	Weight of K_2CO_3 [g]	Weight of Na_2CO_3 [g]	Weight of Lu_2O_3:Eu [g]	Molar ratio of K_2CO_3:Na_2CO_3:$Lu_{1.999}Eu_{0.001}O_3$	Boat material	Fraction taken	Reference
1	10.0199	0.7949	0.7958	72.5:7.5:2	graphite	small	
2	10.0199	0.7949	0.3979	72.5:7.5:1	corundum	small	26
3	10.0199	0.7949	0.3979	72.5:7.5:1	corundum	big	
4	10.3654	0.5299	0.3979	75:5:1	corundum	big	
5	10.3654	0.5299	0.3979	75:5:1	corundum	big	26
6	10.7801	0.2120	0.3979	78:2:1	corundum	big	26
7	10.3654	0.5299	0.3979	75:5:1	corundum	big	
8	10.9873	0.0530	0.3979	79.5:0.5:1	corundum	small	26

Therefore, ligands with a lower electronegativity compared to O^{2-} (χ(O)∼3.4) such as S^{2-} (χ(S)∼2.6) and N^{3-} (χ(N)∼3.0) will lower the energy of the $4f^{N-1}5d^1$ levels, making it more likely for Eu^{2+} to absorb InGaN LED radiation.[10,11] Little work was done on the luminescence of Eu^{2+}/Ce^{3+} in nitrides until Hintzen and co-workers discovered efficient Eu^{2+} emission in Ca^{2+}-α-SiAlON and $M_2Si_5N_8$ (M = Ca^{2+}, Sr^{2+}, Ba^{2+}) that could be excited with violet or blue LEDs.[12,13] One family of efficient phosphors are the $MSi_2O_2N_2$:Eu^{2+} (M = Ca^{2+}, Sr^{2+}, Ba^{2+}) compositions showing emission ranges from ∼498 nm for $BaSi_2O_2N_2$:Eu^{2+} to ∼560 nm for $CaSi_2O_2N_2$:Eu^{2+}.[14,15] For orange and red phosphors, another important family of materials is based upon Eu^{2+}-doped $CaAlSiN_3$ hosts with a distorted wurtzite structure. $CaAlSiN_3$:Eu^{2+} phosphors have a ∼650 nm emission peak and the emission maximum can be tuned down to ∼620 nm by Sr^{2+} substitution by making phosphors using high pressure nitriding of arc-melted alloys.[16,17] The efficient yellow, orange and red Eu^{2+} emission from these nitride phosphors can be combined with YAG:Ce in warm white LEDs for lamps and fixtures that would normally use incandescent lamps or compact fluorescent lamps (CFLs). For example, phosphor blends of YAG:Ce and $CaAlSiN_3$:Eu^{2+} combined with blue LEDs can be used for high CRI (color rendering index), warm white lamps. In addition, it is also possible to use all-nitride phosphor blends to make phosphor-converted (pc)LEDs that cover a full range of CCTs at CRI > 90.[18–20]

As for the sulfides, a very comprehensive review concerning their optical properties and suitability for LED application has been published recently[21] and recent advances in materials, techniques and properties of phosphors in phosphors-converted white light-emitting diodes have been summarized.[22] For example some Eu^{2+}-doped thiosilicates, such as Ca_2SiS_4, $BaSi_2S_5$ and Ba_2SiS_4 can have deep blue to red emissions, which make them applicable in pc-WLEDs. For instance, combining the $CaSiS_4$:Eu^{2+} phosphor with a blue-LED chip (450 nm) gives white light with CCT ∼ 3000 K and CRI ∼ 67.[23] Exploring new types of sulfides with good thermal stability such as thiogallates might be a new direction. Moreover, sulfides with different cation sites may give the solution of wide spectral dispersion in the green and red region. However, sulfide phosphors are in general thermally unstable and sensitive to moisture, which would degrade the luminescence of pc-WLEDs unless phosphor particles are coated with a moisture barrier. The lack of the green emission component when excited by blue-LED chip is another problem which results in low luminous efficacy and low CRI of the pc-WLEDs. These usual objections can be overcome by rather new sulfide family based on rare-earth doped $ALnS_2$ compounds, where A stands for alkali metal (such as Rb, K or Na) and Ln for La, Gd, Lu or Y.[24] Broad Eu^{2+} 5*d*–4*f* emission in some of these sulfides, namely $KLuS_2$ and $NaLuS_2$, is thermally stable at least up to 280°C and 200°C, respectively, with no noticeable moisture sensitivity.[25] Furthermore, it was shown in Ref. 26. that $K_xNa_{1-x}LuS_2$:Eu^{2+} (x = 0–1) samples are not simple mixtures of $KLuS_2$ and $NaLuS_2$, but represent a single phase incorporating both Na and K. Their optical properties make them favorable to use in tunable white LEDs. The crystal structures of $KLuS_2$[27] and $NaLuS_2$,[28] which belong to the α-$NaFeO_2$ structural family, were determined recently. The crystal structures of another potassium rare-earth sulfides have also been determined recently.[29]

This work introduces tunable white light source with tunable CCT temperature based on two different excitation diodes and only single phosphor derived from $K_xNa_{1-x}LuS_2$:Eu^{2+} (x = 0–1) single crystalline sulfides, whose optical properties are described in great details in Ref. 26.

Sample Preparation

The $K_{1-x}Na_xLuS_2$:Eu (0.05%) crystals were prepared in an electric resistance furnace by the chemical reaction of 2N5 H_2S gas with a Lu_2O_3:0.05%Eu (mixture of 5N Lu_2O_3 and 4N Eu_2O_3, equivalent composition is $Lu_{1.999}Eu_{0.001}O_3$) and excess of mixture 4N7 K_2CO_3 and 3N5 Na_2CO_3. The amounts of carbonates and oxides used for the syntheses are summarized in Table I. The chemical reactions were carried out in a 5N saphire tube (Crytur) or 3N corundum tube. The tube was placed in an electric resistance furnace equipped with heating/cooling-rate regulation. The scheme of the set-up was outlined in Ref. 30. Either 5N Ar or 2N5 H_2S gas was allowed to flow into the reaction tube. The gases were taken directly from pressurized cylinders using a three-way stopcock to switch between them.

Prior to the reaction itself, the reagents (K_2CO_3, Na_2CO_3 and $Lu_{1.999}Eu_{0.001}O_3$) were mixed and the mixture homogenized in an agate mortar. The mixture was placed in a 3N corundum boat or high pure graphite boat (graphite boat was used only for synthesis of TS257) and inserted into the sapphire tube or corundum tube (inner volume 0.9 dm^3 for both of them). The mixture was then heated to 1273 K using the electric resistance furnace (heating rate 10 K/min) under a flow of Ar (15 dm^3/hour). After the desired temperature had been reached, the reaction mixture was annealed for 90 min under a flow of H_2S (15 dm^3/hour). Following annealing, the system was cooled under a flow of Ar (1 K/min, 0.3 dm^3/hour). Upon reaching room temperature, the corundum boat (or graphite boat) was removed from the tube and the reaction products were purified by suspension and decantation, three times with distilled water and once with ethanol or acetone. K_2S or Na_2S was removed by water, while $K_{1-x}Na_xLuS_2$:Eu was left behind. The yield was nearly 100%, with any loss attributed to imperfect product separation. The products were stored in small glass flasks under an Ar atmosphere and used for further analysis. Further details about syntheses are reported in Refs. 24,26.

During the $K_{1-x}Na_xLuS_2$:Eu^{2+} (0.05%) preparation two fraction of thin hexagonally shaped crystals are usually obtained which, for the purposes of following work, will be denoted as 'big', meaning the larger platelets with the dimensions up to 3 × 3 × 0.2 mm, and 'small'.

Experimental

The phase composition of the crystalline samples studied was confirmed and the lattice parameters determined via X-ray Powder Diffraction (XRD) using Rigaku MiniFlex 600 diffractometer utilizing Ni-filtered Cu-$K_{\alpha 1,2}$ radiation and NaI:Tl scintillation detector. The samples were measured in Bragg-Brentano geometry in the range of 10° – 80° 2θ using continuous mode (scan speed 2°/min). The lattice parameters of rhombohedral $ALnS_2$ lattice were then determined from the observed positions of diffraction peaks using weighted linear regression. Due to the need to grind samples for this analysis and the

Table II. The measured XRF signal ratios between K and S and the determined lattice parameters of presented $K_{1-x}Na_xLuS_2:Eu^{2+}$ (0.05%) samples; * not measured, for details, see the Experimental setup.

Sample assignment (arbitrary)	Estimated composition	K/S XRF signal ratio	Lattice parameter *a* [Å]	Lattice parameter *c* [Å]	Reference
1 (small)	$K_{0.65}Na_{0.35}LuS_2$	3.08(10)	3.945(5)	21.74(2)	
2 (small)	$K_{0.74}Na_{0.26}LuS_2$	3.52(8)	3.944(3)	21.63(3)	26
3 (big)	$K_{0.75}Na_{0.25}LuS_2$	3.56(8)	n. m.*	n. m.	
4 (big)	$K_{0.80}Na_{0.20}LuS_2$	3.80(8)	n. m.	n. m.	
5 (big)	$K_{0.82}Na_{0.18}LuS_2$	3.86(8)	3.952(5)	21.73(2)	26
6 (big)	$K_{0.85}Na_{0.15}LuS_2$	4.02(6)	3.948(2)	21.79(1)	26
7 (small)	$K_{0.86}Na_{0.14}LuS_2$	4.04(9)	3.952(4)	21.74(1)	
8 (big)	$K_{0.93}Na_{0.07}LuS_2$	4.38(10)	3.957(2)	21.85(1)	26

rather small amount of the big fraction, composition was not verified by powder XRD for each sample, see Table II.

Elemental composition (for elements heavier than Mg) of both crystal fractions was determined using X-ray Fluorescence (XRF) analyzer Niton XL3t 900 GOLDD series (Ag anode) mainly in the Low range of the Cu/Zn Mining mode (X-ray tube voltage 20 kV, current 100 mA). The relative content of K and S in all samples was determined from the peak intensity of their characteristic K_α emission lines (2.31 and 3.15 keV, respectively) after a correction for the interfering Ag-L lines.

Overall emission spectra of constructed circadian source were obtained with Ocean Optics QE65000 spectrometer equipped with a Peltier cooled CCD sensor. The photoluminescence of prepared phosphors was performed on a homemade apparatus. The sample was illuminated by a EQ99X laser driven light source filtered by a Jobin Yvon Gemini 180 monochromator. The exit slit from the monochromator was then reimaged on the sample by two 100 m focal length, 2 inch diameter MgF_2 lenses. The whole apparatus has been calibrated by means of a Newport 918D Low power calibrated photodiode sensor over the range 190–1000 nm. The resolution of the system being 4 nm. The emitted light from the sample is collected by an optical fiber connected to a Jobin-Yvon TRIAX320 monochromator equipped with a cooled CCD detector. At the entrance of the monochromator different long pass filter can be chosen in order to eliminate the excitation light. The resolution of the detection system is 2 nm.

The Device Construction

Presented circadian source with tunable white light emission, a scheme of which is shown in Figure 1, uses two different kinds of commercially available excitation diodes. In this particular device there are three nearUV (380 nm, 1 W power) and one blue (460 nm, 3 W power) excitation diodes, all purchased from GM Electronics company, and an active $K_{1-x}Na_xLuS_2:Eu^{2+}$ (0.05%) phosphor layer. Excitation diodes are in an arrangement allowing all the excitation light released from them to meet in a place where the phosphor layer is placed between two quartz glasses. The diodes and the phosphor are placed in a black light-bulb-like cylinder. The ratio of diodes′ power can be finely and continuously tuned by external electronics. In this way, phosphor can be excited either by the nearUV diode, or by the blue diode but, most interestingly, with both diodes at the same time with variable amplitudes. Tunable white light source can be constructed in this manner using just a single phosphor.

1. circadian light source
2. blue LED
3. nearUV LED
4. blue light emitted by blue LED
5. nearUV light emitted by near UV LED
6. overall white light emitted by circadian source
7. potentiometer
8. blue LED driver
9. nearUV LED driver
10. black tube
11. quartz window with phosphor layer

Phosphors Composition

The measured XRF spectra revealed the presence of K, S and Lu in all the studied samples, while Na-K_α line has a too low energy to be detectable in the apparatus used. Due to a low Eu concentration and the presence of intense diffraction peaks in the spectra (especially in the big fraction), Eu presence could not be observed. No significant elemental impurities were detected. The signal ratio K/S for the fraction of big crystals corresponded very well with the experimentally observed dependence for $K_{1-x}Na_xLuS_2$ on the melt composition obtained in our previous work,[26] whereas the small fraction consistently featured a higher K/S value (see Table II). Thus, the smaller crystals probably contain slightly elevated concentrations of K (on average) in their structure with respect to Na.

The diffraction patterns of the small fraction of $K_{1-x}Na_xLuS_2$ crystals confirmed that the samples contained only the rhombohedral $ALnS_2$ lattice (space group R-3m) with no major phase impurities. Due to the morphology of crystals (very thin hexagonal-shaped platelets), the preferential orientation greatly emphasizes all (0 0 3n) diffraction peaks, complicating phase identification. As the main probable impurity (Lu_2O_2S, usually a fine powder) was not detected in the smaller fraction, its presence in the big fraction consisting of transparent single crystals is virtually impossible. Therefore, the big fraction also contained a pure $ALnS_2$-type phase.

In crystalline materials prepared from the melt containing ~80–91 at. % K (see Table I), the observed diffraction peaks were significantly broadened relative to other samples. As shown in Ref. 26, there is an abrupt change in lattice parameter *c* in this area (the inflexion point of the experimental sigmoidal curve). This broadening most probably indicates a wide variation of lattice parameters in different crystals or a large microstructural strain inside a single crystal. Therefore, the determined lattice parameters of such samples represent only their mean value with significant uncertainties.

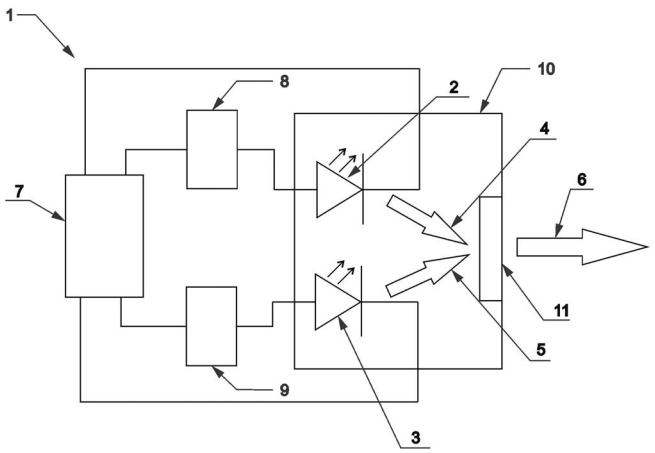

Figure 1. A scheme of circadian light source.

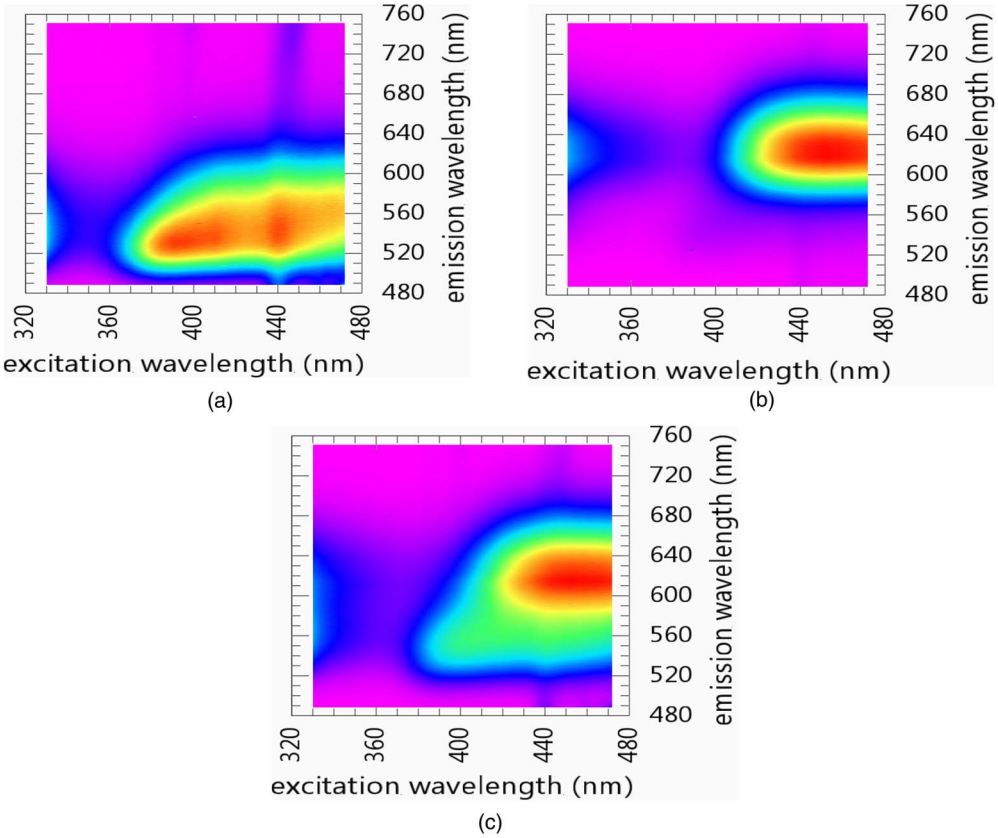

Figure 2. a. PL/PLE contour plot of the $K_{0.93}Na_{0.07}LuS_2:Eu^{2+}$ (0.05%, big fraction). b. PL/PLE contour plot of the $K_{0.75}Na_{0.25}LuS_2:Eu^{2+}$(0.05%, big fraction). c. PL/PLE contour plot of the $K_{0.82}Na_{0.18}LuS_2:Eu^{2+}$ (0.05%, big fraction).

Optical Properties

To demonstrate that broad excitation and emission wavelength region can be covered by a single $K_{1-x}Na_xLuS_2:Eu^{2+}$ (0.05%) phosphor of a given composition (Table II), RT PL and PLE spectra of the phosphors were recorded using CCD camera. Three limit cases are observed:

For the $K_{1-x}Na_xLuS_2:Eu^{2+}$ (0.05%) samples containing low amount of sodium, mainly the emission in green and yellow spectral region is obtained as seen in Figure 2a. Such emission can be well excited in the 360–480 nm region. For higher sodium concentration in $K_{1-x}Na_xLuS_2:Eu^{2+}$ (0.05%), emission in red part is present, which can be excited in the 400–480 nm region (Figure 2b). Finally, the most interestingly for LEDs application, for certain sodium and potassium ratios, extraordinarily broad emission in the 510–710 nm spectral region is visible under the 370–480 nm excitation, see Figure 2c.

As an example, selection of overall emission spectra of the presented circadian light source using $K_{0.8}Na_{0.2}LuS_2:Eu^{2+}$ (0.05%, big fraction) phosphor is displayed in Figure 3. The spectra were measured with different intensity ratios between nearUV and blue diode. In Figure 3a, the blue diode is fixed to 5% of its power and in Figure 3b, the nearUV diode is fixed to 10% of its power. There are three

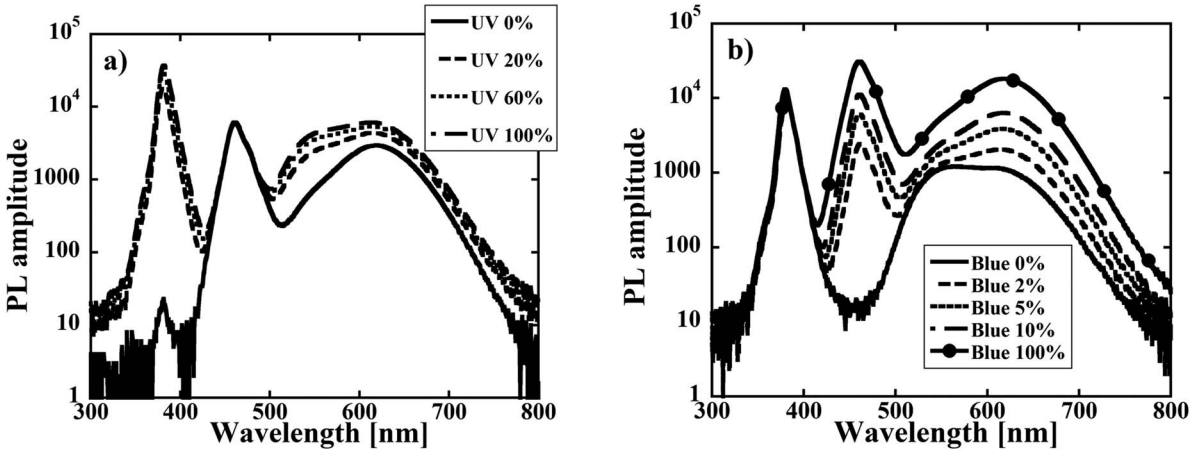

Figure 3. Examples of overall emission spectra of circadian light source with different ratios of nearUV and blue diodes using $K_{0.8}Na_{0.2}LuS_2:Eu^{2+}$ (0.05%, big fraction) phosphor; a) blue diodes fixed to 5% of its power; b) nearUV diode fixed to 10% of its power.

differentiable spectral features to be noted in all spectra in Figure 3. At the higher energy side, the emission from the near UV diode peaking at around 380 nm can be seen. The emission of the blue diode at 455 nm is present as well. Finally, visible phosphor luminescence is observed at the low energy side. It can be seen from Figure 3 that different nearUV and blue diode intensity ratios give rise to different emission spectra in the 480–800 nm region. As a result, the combined overall emission spectra differ in their CIE coordinates and therefore, CCT temperatures vary as well. It should be noted that having the nearUV diodes intensity fixed and varying the blue one offers higher tunability range as will be discussed below.

Tunability of The Output White Light

To show the tuning capabilities of the device, the output spectra for each sample were measured for different combinations of nearUV and blue excitation. Excitation from 0 to 100% was set for both excitation sources independently and the resulting spectra were recorded and processed (usually steps of 10–20% were made).

For each spectrum, the CIE-xy color coordinates and CCT were calculated using CIE 1931 specification, and the change of the coordinates was observed for constant excitation power of nearUV or blue.

To compare the obtained light from the perspective of color rendering, CRI (color rendering index) and CQS (color quality scale) values were calculated.[31–33] These values represent the ability of a light source to reproduce the perceived color of some object as close as possible to the object's color under natural standard illumination. The bigger the value is, the better the reproduction is. The CRI specification was designed to compare mainly incandescent light sources to natural white light (which has CRI = 100). However, using CRI on LED-based light sources can lead to inaccurate results, e.g. a LED with CRI = 25 can actually produces more vivid colors of the illuminated object. In comparison, the newer CQS metric uses more color etalons to evaluate, the computation is also improved to provide better results for LEDs than the CRI metric.[31]

Analysis of the measured spectra answers the following questions:

1) Do we need to change both excitation intensities, or is changing only one of them and keeping the other fixed at some value enough to provide good light source tunability?
2) What is the actual needed nearUV excitation intensity–do we need full 100% of the available power, or is e.g. 50% enough?
3) What are the available tuning areas for our samples?

In construction of a real device, its complexity has noticeable influence on the final product price. Thus we wanted to figure out, if it is really needed to control both excitation sources, or if it is possible to fixate one excitation on a certain level and use only the other to control the output properties. Figure 4 shows "areas of tunability"–color reachable by changing the level of blue excitation for fixed nearUV excitation–for six samples and selected nearUV excitation level. We can see that using variable blue excitation covers very broad range of colors, in different parts of the spectrum for different samples. When blue excitation is held constant, the area of tunability is much smaller and is also moving significantly in the CIE diagram. In comparison, the tunability when nearUV is held constant does not change much, almost preserving the range of tunability in most cases. We conclude that targeting for broad tunability range is better with constant nearUV excitation. In contrary, if more precision and less output sensitivity are required, it would be better done with constant blue excitation.

As shown in Figure 4, full nearUV excitation is not always needed. This factor is important because the nearUV excitation does not contribute to the visible spectrum and the overall excitation effectiveness when using nearUV is lower than in the case of blue excitation. Actually, the nearUV fixed values were chosen to represent the sample in Figure 4, other measured series with more nearUV excitation are very similar–there is no real benefit from using full nearUV excitation because of higher energy consumption.

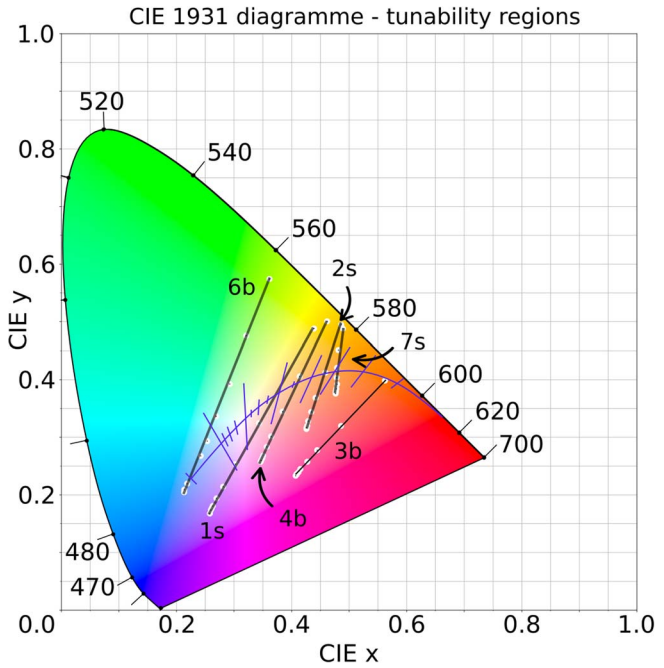

Figure 4. The tunability regions of the samples for selected constant nearUV excitation intensity (indicated in brackets) and 0,2,5,10,20,40,60,80,100% of blue excitation. Samples presented are 6b = $K_{0.85}Na_{0.15}LuS_2:Eu^{2+}$ (0.05%, big fraction, 40% nearUV), 1s = $K_{0.65}Na_{0.35}LuS_2:Eu^{2+}$ (0.05%, small fraction, 100% nearUV), 4b = $K_{0.8}Na_{0.2}LuS_2:Eu^{2+}$ (0.05%, big fraction, 60% nearUV), 3b = $K_{0.75}Na_{0.25}LuS_2:Eu^{2+}$ (0.05%, big fraction, 60% nearUV), 7s = $K_{0.86}Na_{0.14}LuS_2:Eu^{2+}$ (0.05%, small fraction, 40% nearUV), 2s = $K_{0.74}Na_{0.26}LuS_2:Eu^{2+}$ (0.05%, small fraction, 60% nearUV). Variable excitation produces color across a broad range of the spectrum and also near the white point (x,y = 0.33,0.33); b stands for big, s far small, see also Table II.

Measured spectra are usually expressed using the CCT value. This value can be calculated only near the line of white light sources, so for some spectra, the CCT cannot be even determined. To quantify the usability of the created output light, CRI and CQS were calculated. The data for the best spectra is shown in Table III. The resulting light will be perceived as white enough when it is not too far from the black body locus (BBL, shown in Figure 4). This is usually measured by units based on MacAdam ellipses. Because calculating the "MacAdam distance" is discouraged by,[34] we used the commercial "binning" scheme from OSRAM based on 3-step MacAdam ellipses.

Since the measured points were chosen to explore the whole tunability, we could hit the BBL line only by coincidence. The real tunable white light range for one sample (i. e. one line in Figure 4) can be defined as a part of the BBL line around the intersection of the tunability sample line with the BBL line. We have found 4 such intersections, calculated the relevant CCT and using the mentioned binning scheme[35] the range of CCT which would be in one bin band (i.e. not further than 4-step MacAdam ellipses from the BBL) was estimated. The results are show in Table IV, where the value of tunability means the width of the CCT interval around the center CCT point.

The tunability might seem small which is given by the nature of the excitation-emission dependence. By mixing the $K_{0.86}Na_{0.14}LuS_2$ (small fraction) and $K_{0.85}Na_{0.15}LuS_2$ (big fraction) samples, it might be possible to obtain a tunability line that will be close to the BBL in the 2700 K-5000 K region. Such light source might still not be good enough for applications where color fidelity is required. However for a circadian light source this could work well thanks to the adapting nature of the human vision system.

To sum up, output light with CCT from 2500 K to 8000 K (or even more) was obtained, the best CRI is 87.2 for sample $K_{0.65}Na_{0.35}LuS_2:Eu^{2+}$ (0.05%, excitation nearUV 100%, blue 2%).

Table III. The best output light results obtained with CRI or CQS; *for sample composition see Table II.

Sample∗	Near UV [%]	Blue [%]	CIE-x	CIE-y	CQS	CRI	CCT
1 (small)	40	2	0.331	0.296	82.5	82.3	5595
1 (small)	60	2	0.338	0.308	82.4	84.6	5197
1 (small)	80	2	0.343	0.316	82.4	86.1	4970
1 (small)	100	2	0.350	0.327	82.2	87.2	4722
1 (small)	20	2	0.317	0.272	81.4	75.0	6840
1 (small)	100	5	0.309	0.258	80.2	70.6	8019
2 (small)	100	2	0.467	0.423	78.8	81.2	2704
2 (small)	80	2	0.464	0.418	78.7	82.0	2691
2 (small)	60	2	0.462	0.413	78.5	82.5	2681
2 (small)	40	2	0.460	0.407	78.3	83.0	2671
2 (small)	20	2	0.453	0.392	77.3	83.3	2635
2 (small)	100	5	0.451	0.382	76.4	82.6	2591
4 (big)	10	2	0.388	0.343	76.0	82.8	3507
2 (small)	10	2	0.446	0.374	75.9	80.9	2587
2 (small)	80	5	0.448	0.375	75.7	81.5	2567
4 (big)	20	2	0.404	0.375	75.6	80.3	3420
4 (big)	20	5	0.376	0.316	75.6	80.6	3607
4 (big)	40	5	0.385	0.337	75.6	82.7	3536
4 (big)	60	5	0.390	0.347	75.5	82.8	3508
4 (big)	80	5	0.393	0.355	75.4	82.3	3483
4 (big)	100	5	0.398	0.364	75.3	81.2	3462
4 (big)	80	10	0.373	0.311	75.3	80.4	3655
2 (small)	60	5	0.446	0.371	75.2	80.6	2550
4 (big)	100	10	0.377	0.320	75.1	81.5	3615

The best CQS metric is 82.5 for sample $K_{0.65}Na_{0.35}LuS_2:Eu^{2+}$ (0.05%, excitation nearUV 40%, blue 2%). The tunability of the output light was demonstrated for cold and warm white color and future improvement using phosphor mixing is proposed. For better demonstration, the best obtained spectrum is shown in Figure 5: The peak value of nearUV excitation is cropped to show the visible spectrum in detail; the inset with the rendering quality of all fifteen CQS color samples shows almost perfect rendering of the green-yellow color, while orange and green-blue colors perform worse (10 out of 15 color samples have CQS > 80).

Quantum yield of as prepared phosphors can be roughly estimated from the temperature dependence of the Eu^{2+} ns decay time and the Eu^{2+} emission intensity. As both do not change significantly within a certain temperature range, which is our case (see[25,36]), quantum yield in the first approximation can be estimated to be close to unity. Certainly, during rather complicated sample preparation, some parasitic absorption lowering the real quantum yield could be expected and therefore additional experiments will have to be provided in future research. Thermal losses as well as losses due to the Eu^{2+} re-absorption can be estimated from the Stokes shift. However, taking into account the Stokes shift of $YAG:Ce^{3+}$, which is approximately 500 meV, and the Stokes shift of our phosphor for limited composition $KLuS_2:Eu^{2+}$, which can be estimated roughly as 430 meV (if we consider the lowest Eu^{2+} 4*f*–5*d* absorption band to be at around 440 nm[36]), we can guess that thermal recombination losses will be comparable for both these phosphors.[25,36] The quantum efficiency of $YAG:Ce^{3+}$ under blue LED excitation is >85% even at 200°C.[37] Furthermore, both Ce^{3+} and Eu^{2+} ions exhibit 5*d*–4*f* luminescence so the absorption and emission transitions are parity and spin allowed, giving strong absorption of blue LEDs and rather fast decay time that prevents saturation quenching.

Table IV. Tunability values of chosen samples.

Sample	CIE_x	CIE_y	CCT [K]	Tunability [K]
$K_{0.65}Na_{0.35}LuS_2$ (small)	0.37	0.373	4280	400
$K_{0.80}Na_{0.20}LuS_2$ (big)	0.41	0.394	3440	250
$K_{0.74}Na_{0.26}LuS_2$ (small)	0.456	0.41	2750	100
$K_{0.86}Na_{0.14}LuS_2$ (small)	0.48	0.414	2460	100

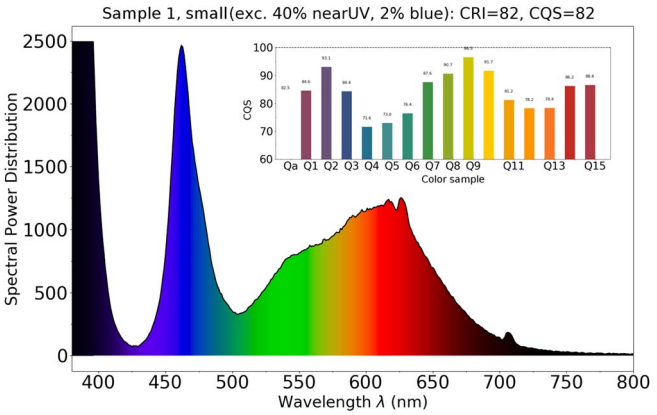

Figure 5. Obtained mixed spectrum with highest CQS metric from sample $K_{0.65}Na_{0.35}LuS_2:Eu^{2+}$ (0.05%) under mixed excitation (nearUV 40%, blue 2%). The nearUV peak is cropped to show the visible spectrum in detail. The inset shows rendering of all 15 CQS color samples numerically illuminated with the experimental spectrum. 10 out of 15 samples have CQS > 80, maximum value is 97). The color of the bars represents the rendering of the samples under the standard D65 illuminant.

Based on these comments we believe we can, very conservatively, consider the quantum efficiency of our Eu^{2+}-doped $K_xNa_{1-x}LuS_2$ to be comparable to that of $YAG:Ce^{3+}$, at least up to 500 K.[25] Naturally, the Stokes losses of Eu^{2+}-doped $K_xNa_{1-x}LuS_2$ for nearUV excitation (390 nm) will increase compared to that in the blue spectral range. However, $YAG:Ce^{3+}$ cannot be excited in this wavelength region at all due to the absence of Ce^{3+} absorption bands. This provides strong comparative advantage to our sulfide phosphor presented here.

Conclusions

A set of single-crystalline platelets of Eu^{2+}-doped $K_xNa_{1-x}LuS_2$ phosphors (x = 0–1) has been successfully synthesized. XRD confirmed the presence of a single crystalline phase, while the X-ray fluorescence technique was used to determine the actual phosphor composition. The given phosphors, together with commercially available excitation diodes of two kinds (nearUV and blue), have been used to construct a real functional demonstration device representing the source of white light with tunable CCT temperature. PL/PLE contour plots of selected phosphors show the maximally available usable spectral range which, for the best sample, covers extraordinarily broad emission of Eu^{2+} 5*d* - 4*f* in the 510–750 nm spectral region under the 360–470 nm excitation. Overall emission spectra of a functional demonstration device with given phosphor prove the tunability in a large area of color space and show the limits of nearUV and blue diodes′ power to obtain demanded white light output with CCT from 2500 K to 8000 K (or even more). The best CRI is 87.2 for sample $K_{0.65}Na_{0.35}LuS_2:Eu^{2+}$ (0.05%, excitation nearUV 100%, blue 2%) and the best CQS metric is 82.5 for sample $K_{0.65}Na_{0.35}LuS_2:Eu^{2+}$ (0.05%, excitation nearUV 40%, blue 2%). The tunability of the output light was demonstrated for cold and warm white color, with white light tunability region of 100 K to 500 K for the respective samples interpolated on the black body locus (BBL) line. A combination of phosphors is proposed to further improve the white light tuning capabilities. Therefore high application potential of given device is demonstrated for tunable color temperature white LED sources.

Acknowledgments

The financial support of the Technological agency CR, program GAMA, project no. TG02010056 and EC H2020, ASCIMAT project, no. 690599, are gratefully acknowledged.

References

1. V. K. Khanna, *Fundamentals of solid-state lighting: LEDs, OLEDs, and their applications in illumination and displays*, p. 563, CRC Press, Taylor & Francis Group, Boca Raton, (2014).
2. A. Bergh, G. Craford, A. Duggal, and R. Haitz, *Physics Today*, **54**, 42 (2001).
3. J. R. Brodrick and C. E. Christy, in I. T. Ferguson, N. Narendran, S. P. DenBaars, and J. C. Carrano, Editors, p. 1 (2004).
4. A. Žukauskas, M. Shur, and R. Gaska, *Introduction to solid-state lighting*, p. 207, J. Wiley, New York, (2002).
5. G. Zissis, in *LEDs for Lighting Applications*, P. Mottier, Editor, p. 1, ISTE, London, UK (2009).
6. E. F. Schubert, *Light-Emitting Diodes*, Cambridge University Press, Leiden, (2006) http://www.SLQ.eblib.com.au/patron/FullRecord.aspx?p=321244.
7. http://luxreview.com/article/2016/05/two-minute-eplainer-tunable-white-leds.
8. https://www.helvar.com/en/solutions/solutions-for-luminaires/tunable-white-led-products/.
9. https://crowdyhouse.com/shop/nanoleaf-aurora/.
10. P. Dorenbos, *Physical Review B*, **65** (2002).
11. P. Dorenbos, *Physical Review B*, **64** (2001).
12. J. W. H. van Krevel, J. W. T. van Rutten, H. Mandal, H. T. Hintzen, and R. Metselaar, *Journal of Solid State Chemistry*, **165**, 19 (2002).
13. Y. Q. Li et al., *Journal of Alloys and Compounds*, **417**, 273 (2006).
14. Y. Q. Li, A. C. A. Delsing, G. de With, and H. T. Hintzen, *Chemistry of Materials*, **17**, 3242 (2005).
15. V. Bachmann, T. Jüstel, A. Meijerink, C. Ronda, and P. J. Schmidt, *Journal of Luminescence*, **121**, 441 (2006).
16. K. Uheda et al., *Electrochemical and Solid-State Letters*, **9**, H22 (2006).
17. H. Watanabe, M. Imai, and N. Kijima, *Journal of the American Ceramic Society*, **92**, 641 (2009).
18. R. Mueller-Mach et al., *physica status solidi (a)*, **202**, 1727 (2005).
19. N. Kimura et al., *Applied Physics Letters*, **90**, 051109 (2007).
20. https://www.electrochem.org/dl/interface/wtr/wtr09/wtr09_p032-036.pdf
21. P. F. Smet, I. Moreels, Z. Hens, and D. Poelman, *Materials*, **3**, 2834 (2010).
22. S. Ye, F. Xiao, Y. X. Pan, Y. Y. Ma, and Q. Y. Zhang, *Materials Science and Engineering: R: Reports*, **71**, 1 (2010).
23. P. F. Smet, K. Korthout, J. E. Van Haecke, and D. Poelman, *Materials Science and Engineering: B*, **146**, 264 (2008).
24. V. Jarý et al., *Journal of Luminescence*, **170**, 718 (2016).
25. V. Jarý et al., *Materials*, **8**, 6978 (2015).
26. L. Havlák et al., *Materials & Design*, **106**, 363 (2016).
27. J. Fábry et al., *Acta Crystallographica Section B Structural Science, Crystal Engineering and Materials*, **70**, 360 (2014).
28. J. Fábry, L. Havlák, M. Kučeráková, and M. Dušek, *Acta Crystallographica Section C Structural Chemistry*, **70**, 533 (2014).
29. L. Havlák, J. Fábry, M. Henriques, and M. Dušek, *Acta Crystallographica Section C Structural Chemistry*, **71**, 623 (2015).
30. L. Havlák, V. Jarý, M. Nikl, P. Boháček, and J. Bárta, *Acta Materialia*, **59**, 6219 (2011).
31. W. Davis, *Optical Engineering*, **49**, 033602 (2010).
32. M. Rejman, V. Babin, R. Kucerková, and M. Nikl, *Journal of Luminescence*, **187**, 20 (2017).
33. http://colour-science.org/.
34. Technical Note CIE TN 001:2014: Chromaticity Difference Specification for Light Sources.
35. https://ledlight.osram-os.com/wp-content/uploads/2013/01/OSRAM-OS_LED-FUNDAMENTALS_Colorimetry_v1_07-11-11_SCRIPT.pdf.
36. V. Jarý, L. Havlák, J. Bárta, E. Mihóková, and M. Nikl, *Chemical Physics Letters*, **574**, 61 (2013).
37. V. Bachmann, C. Ronda, and A. Meijerink, *Chemistry of Materials*, **21**, 2077 (2009).